JOURNAL OF MATERIALS SCIENCE **34** (1999) 607–614

The effect of dispersed paint particles on the mechanical properties of rubber toughened polypropylene composites

R. T. QUAZI, S. N. BHATTACHARYA, E. KOSIOR
Department of Chemical and Metallurgical Engineering and CRC for polymers, Royal Melbourne Institute of Technology, Melbourne, Victoria, Australia
E-mail: rchsb@rmit.edu.au

The influence of dispersed paint particles on the mechanical properties of rubber toughened PP was investigated. The matrix was basically a hybrid of PP, rubber and talc. Model systems with spherical glass bead filled matrix were also studied to examine the effect of filler shape and size. Properties like tensile strength, strain at break, impact strength, and fracture toughness were influenced by the dispersed inclusions. Tensile strength at yield decreased linearly according to Piggott and Leinder's equation. Strain at break decreased more drastically with paint particles than glass beads, revealing that irregularly shaped particles offered greater stress concentrations. The tensile strength and strain at break were less influenced by the size of paint particles whereas a slight decrease in the modulus values was observed with decreasing particle size. Impact strength and fracture toughness also decreased with increasing filler fraction. Lack of stress transfer between filler and matrix aided in reduction of impact strength. Decrease in fracture toughness was influenced by volume replacement and constraints posed by fillers. The size of paint particles had little effect on the impact strength and fracture properties at the filler concentration levels used in this investigation.

1. Introduction

With new polymerization processes introduced in the last decade, polypropylene (PP) has become one of the most favourable materials for use in low cost composites and blends. Polypropylene composites have wide applications in motor and household industries, and components made from these materials are expected to have good impact strength or toughness and to withstand a wide temperature range. Meanwhile, waste minimization programs are encouraging the automotive industries to recycle their plastic parts. PP bumpers are targeted for recycling because of their large volume and relatively simple material composition. Most of these bumpers are coated with polyurethane based paint which becomes dispersed into the matrix during reprocessing, influencing the material properties. In previous works [1, 2] some mechanical and rheological properties of the recycled painted PP bumpers have been examined but the fracture behaviour has not been looked into, which is the theme of this investigation. Though much work has been done on the fracture behaviour of particulate filled polymers with brittle matrices such as poly(methyl methacrylate), epoxy and polyester resins, tough materials which normally exhibit plasticity prior to fracture, such as polypropylene, have not been covered widely. In most of the previous investigations, fillers such as glass beads, silica particles, talc, mica and calcium carbonate were incorporated with polypropylene to observe the fracture behaviour of the systems [3–11]. Factors such as shape and size of fillers, particle volume fraction and filler-matrix adhesion were considered as variables. Some work has been performed with PP/elastomer/inorganic filler (talc, calcium carbonate, magnesium hydroxide) to observe the effect of phase morphology, interfacial adhesion and filler particle shape and volume fraction on the tensile properties and fracture toughness of PP [12–15].

The present work is concerned with the tensile and fracture properties of the PP/rubber/filler composites corresponding to bumper materials. Deformation behaviour of the composites were studied through tensile and flexural tests. Fracture studies were performed on an instrumented impact tester with sharply notched Charpy specimens. Electron microscopy revealed the matrix nature after fracture.

2. Experimental study

2.1. Materials

The materials used for the base matrix were: polypropylene copolymer (LYM 120) (ICI Plastics, Australia) with a melt flow index of 14 g/10 min (230 °C, 2.16 kg); polyolefinic elastomer VM 42E (Kemcor, Australia) with a melt flow index of 2 g/10 min (230 °C, 5 kg); and a commercial grade talc, TALC TX (Commercial

TABLE I Average particle size and densities of the fillers

	Size range (sieve analysis) (μm)	d (μm)	ρ (kg/m^3)
Talc		8	2650
Paint particles	150-106	135	1770
	75-53	63	1770
Glass beads	106-53	66	2500

Minerals Limited, Australia) with a specific surface area of 0.9 m^2/g (chemically untreated). A step by step procedure was followed to obtain the irregularly shaped ground paint particles for use in the blends. First, some polypropylene sheets were cleaned and then painted with three layers of paint: primer (a chlorinated polyolefin), base coat (a polyester) and clear coat (two pack polyurethane coating) as found on car bumpers. The reaction between polyisocyanate and polyol in the two pack polyurethane coating means curing of the material on the substrate to give the final paint film. These sheets were baked in the oven at 80 °C for 30 minutes to allow the paint to set. The paint was then scraped from the sheets manually with a scraper as thin layers and ground, first in a mixer and finally in a ring grinder. The ground paint was sieved to different sizes, and particles of size 150-106 and 75-53 microns were used with the blends as fillers. Solid spherical glass beads were obtained from Potters Industries Inc., Australia.

The average volume mean diameter (d) of the fillers was determined using a Malvern Mastersizer X and the densities of the materials were measured using a pycnometer at room temperature. The size range, particle diameter (d) and densities (ρ) of the fillers are shown in Table I.

2.2. Preparation of composites and moulding

Model blends were prepared with PP/rubber/talc, incorporating irregular paint particles and solid glass beads into them. Glass bead systems were examined to find the effect of filler shape. The base matrix PP/rubber (20 wt %)/talc (10 wt %) was dispersed with two sizes of paint particles ranging from 1–9% by weight (0.54-5 vol %) and glass beads ranging from 1–22% by weight (0.38-10 vol %). Composites were prepared first by tumble mixing preweighed quantities of all the components and filler, followed by compounding on a twin screw extruder. The melt temperature was kept at 200 °C and screw speed was 60 r.p.m. The extrudates were then granulated for injection moulding of test pieces. Each of the composites were moulded into tensile and flexural bars. The volume fraction (V_i) of the composites were calculated from weight fractions (W_i) using the following relationship:

$$V_i = \frac{\frac{W_i}{\rho_i}}{\left(\sum_{i=1}^{n} \frac{W_i}{\rho_i}\right)} \quad (1)$$

where ρ_i is the density of any component i.

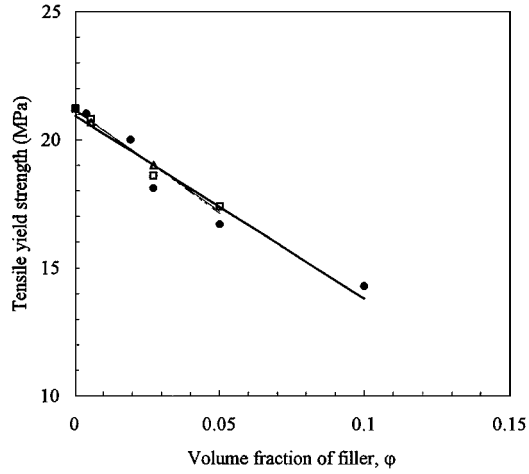

Figure 1 Tensile yield strength versus volume fraction of (●) glass bead, (□) paint (63 μm) and (Δ) paint (135 μm) filled PP/rubber/talc system.

3. Results and discussion

3.1. Tensile tests

As a starting point, it is assumed that the base matrix PP/rubber/talc is a homogeneous mixture, and the paint particles and glass beads added are the second phase of the composites. Then, in principle, it should be possible to calculate the properties of the multiphase materials in terms of the properties of its constituents. Tensile tests were carried on dumbbell shaped specimens with an Instron testing machine at room temperature and at a crosshead speed of 50 mm/min. The specimens were approximately 3 mm thick with a width and gauge length of 10 and 76.8 mm respectively. At least five specimens were tested for each composite. All composites showed a typical yield point from which tensile yield strength at maximum load, σ_y, was calculated. Other quantities such as elongation at break, strain at break and Young's modulus were also measured. All these were then plotted as a function of paint particles and glass beads content, φ.

Fig. 1 shows the effect of filler content on tensile yield strength where the standard deviation was between 0.1 and 0.6. Plots revealed that strength decreased linearly with increasing filler volume fraction. The behaviour was similar to the prediction of Piggott and Leinder [16] for particulate filled systems presented as:

$$\sigma_f = A\sigma_m - B\varphi \quad (2)$$

where σ_f and σ_m are the yield strength of the composite and the matrix respectively, A is the stress concentration factor and B is a constant dependent upon the filler matrix adhesion. As shown in Table II, the values of A and B are not significantly affected by the different filler shapes for the concentration levels used in this

TABLE II Constant values for Piggott and Leinder equation

Filler	A	B
glass (66 μm)	0.99	71.12
paint (63 μm)	0.99	78.90
paint (135 μm)	0.99	81.20

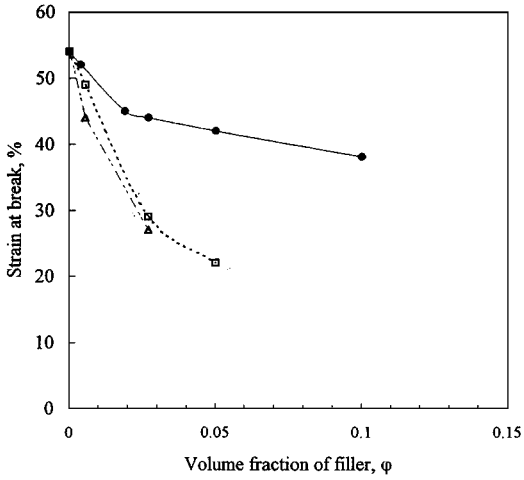

Figure 2 Percentage strain at break versus volume fraction of (●) glass bead, (□) paint (63 μm) and (Δ) paint (135 μm) filled PP/rubber/talc system.

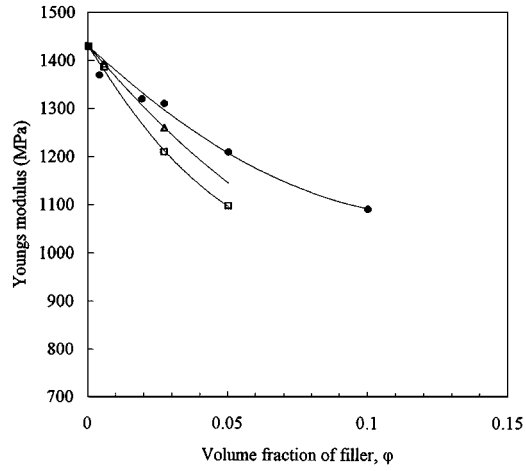

Figure 3 Young's modulus versus volume fraction of (●) glass bead, (□) paint (63 μm) and (Δ) paint (135 μm) filled PP/rubber/talc system.

work. The reduction in strength with increasing filler content suggests that the paint particles and glass beads tend to debond from the matrix upon loading, and as a result the volume fraction of matrix carrying the load falls. Tensile strength is determined at relatively high deformations where any weakness is magnified, reducing in the process of stress transfer. In this case there is no stress transfer and poor adhesion between filler and matrix, both reducing the strength of the composites.

Fig. 2 shows the influence of φ on the strain at break (%) where the standard deviation was between 1 and 5 for the blends. The strain at break showed a decrease with increase in φ, the decrease being quite significant at low filler levels for paint particles (up to 2.7%) and slow with further addition. For glass beads the strain at break dropped gradually throughout. The reduction in elongation of the matrix by the addition of paint and glass implies that an interference is posed by the latter on the deformability of the matrix by introducing mechanical restraint. Irregularly shaped paint particles offered greater stress concentration than spherical glass beads, thus reducing the strain more drastically. The smaller sized paint particles had slightly higher values compared to the larger particles.

The Young's modulus also showed a decrease as φ was increased (Fig. 3) (standard deviation between 10 to 60 for the composites) implying that the addition of inclusions into the matrix formed a weak structure. Possibly the presence of talc in the base matrix played a role in such behaviour. The composite modulus would be governed by the talc particles as it has much higher rigidity (modulus 170 GPa) compared to paint particles (modulus 887 MPa) and glass beads (modulus 73 GPa). So dispersion of the second phase into the base matrix showed a detrimental effect on modulus instead of reinforcing. The modulus values also decreased slightly with decreasing particle size for the paint particles.

The literature indicated that increased adhesion between filler and matrix improved these properties because of higher wettability of the filler with the matrix. Silane based bonding agents were used for glass filled composites [17] and coupling agents were used for mica, talc, calcium carbonate [9–11, 17–19] and silver powder [20] filled composites, which seem to plasticize/lubricate the matrix thus improving the properties. No comments can be made on improvement of the properties for the composites under study as the use of bonding or coupling agents for the dispersed phase was beyond the scope of the present investigation.

3.2. Flexural tests

Three point bend flexural strength and modulus were determined by testing flexural bars of dimensions $126 \times 13 \times 3$ mm at a crosshead displacement rate of 10 mm/min on an Instron testing machine. None of the specimens failed under this mode. Modulus and strength were computed from the initial slope and maximum load on the trace respectively. The modulus showed a decrease in value with increasing φ as shown in Fig. 4 which can be explained as in the above section.

3.3. Impact strength

Notched impact strength as a function of glass bead and paint content was measured using Izod impact

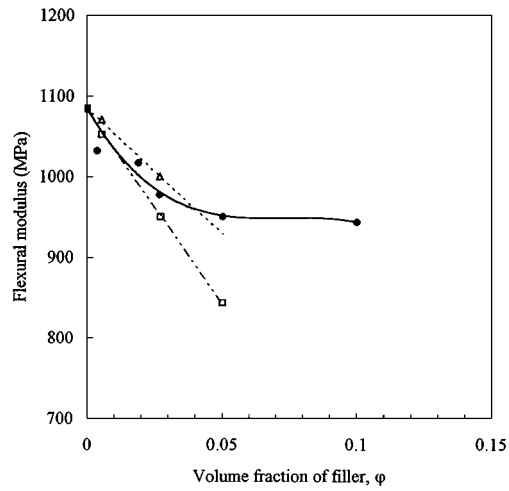

Figure 4 Flexural modulus versus volume fraction of (●) glass bead, (□) paint (63 μm) and (Δ) paint (135 μm) filled PP/rubber/talc system.

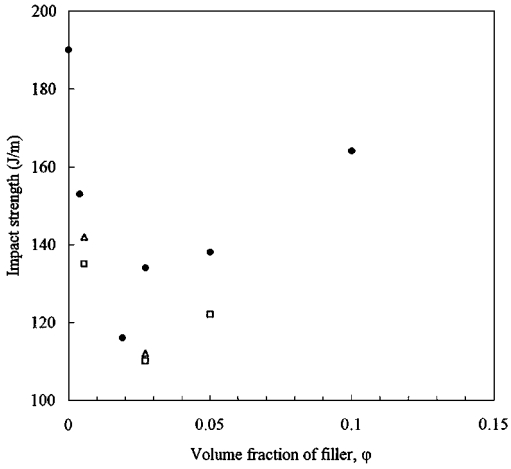

Figure 5 Impact strength versus volume fraction of (●) glass bead, (□) paint (63 μm) and (△) paint (135 μm) filled PP/rubber/talc system.

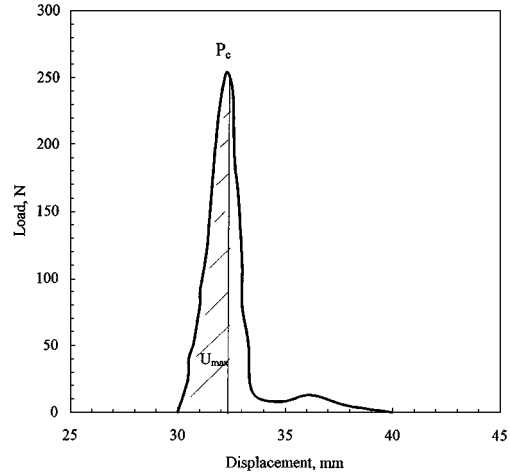

Figure 6 Typical load displacement diagram for PP/rubber/talc composites filled with paint particles.

specimens of thickness (B) and depth (D) of 3 and 13 mm respectively. A Davenport Izod Impact tester was used to perform the impact tests at room temperature. It is a pendulum type machine where a notched specimen is broken by a blow of known energy from the pendulum. The loss of pendulum energy equals the impact strength of the test specimen, and is indicated by the movement of a pointer on a calibration scale. The effect of filler content on impact energy per specimen thickness is shown in Fig. 5, where each datum represents the average of five to eight measurements and the standard deviation was between 3 to 18. A clear drop in impact energy is observed with increase in φ. The reduction is explained by the poor interface between the matrix and the filler, which is evident from the fractography of the broken specimens. Lack of stress transfer between filler-polymer also aids the impact failure. The filler particles act as stress concentrators and crack propagators, weakening the matrix. It is worth noting that with higher glass bead concentration (i.e. 10% volume) the impact strength tends to increase slightly again. The observation was similar to that of Volenberg and Heikens [21] who worked with chalk filled PP and observed that in the case of excellently adhering chalk particles, an increase in filler content decreased the impact strength, whereas in the case of poor adhesion, a maximum in impact strength was observed at a certain volume fraction of filler. The occurrence of the maximum value as explained by the authors was due to a combination of two shearing processes: diffuse shearing and the formation of shear bands observed by a slow tensile test. Although in this study the 10% glass bead showed the highest value in strength, it is not possible to conclude whether further increase in strength was possible by increasing dispersed phase concentration above 10%.

3.4. Fracture tests

Fracture tests were performed on Charpy specimens of dimensions the same as the Izod samples, with notch length varying from 0.7 to 5.7 mm. The notches were sharpened by slowly pushing a razor blade through them. The distance between the supports ($2L$) was 51.28 mm. Fracture tests were conducted at room temperature with an instrumented impact tester (IIT) ITR 2000, equipped with the Charpy anvil. In this study, the striker velocity was 3.4 m/s. During the test a force transducer continuously monitors the load of the impactor, while the displacement transducer monitors the distance the impactor has travelled. Subsequent analysis of the force versus displacement data carried out by the computer produces the required information. A typical load versus displacement curve obtained in this study is shown in Fig. 6, where the fracture load (P_c) is given by the peak load of the curve and the area under the curve up to that point ($U_{\max}$) is taken as the energy required to initiate the crack.

From the fracture mechanics analysis, the impact fracture energy G_c can be determined using the following equation given by Plati and Williams [22]:

$$U_{\max} = U_T + G_c B D \phi \tag{3}$$

where $U_{\max}$ is the impact energy absorbed upto maximum load, U_T is the kinetic energy loss, ϕ is a geometrical factor defined as:

$$\phi = C/[dC/d(a/D)] \tag{4}$$

and C is the compliance of the cracked sample. The values of ϕ is tabulated as a function of a/D and $2L/D$ for Charpy specimens in [22].

The plot of $U_{\max}$ versus $BD\phi$ for the composites as shown in Fig. 7 was non-linear, revealing that brittle failure was not observed and plasticity effect occurred. The fractured surfaces showed a small whitened plastic zone ($2r_p$) ahead of the crack tip and the failure can be classified as semi-brittle in nature. It is assumed that with a small plastic zone, the elastic stress field around the crack tip is not greatly disturbed and the extent of the plastic zone may be defined by the elastic stresses. Irwin [23] suggested that the effect of crack tip plasticity may be approximated by adding the radius of circular plastic zone, r_p, to the original crack length a. The tip of the crack is thus at the centre of

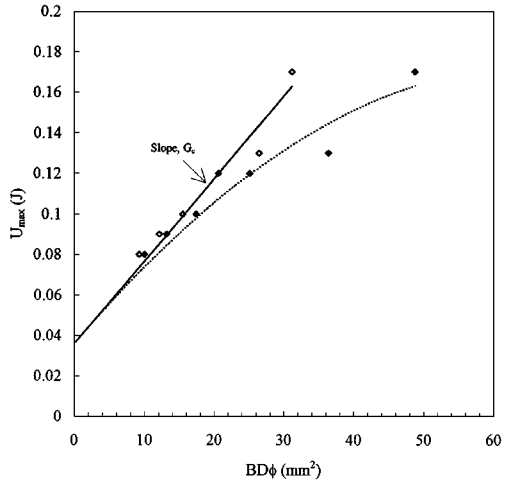

Figure 7 Impact fracture energy (U_{max}) plotted against BDϕ for 2.7% paint (63 μm) in PP/rubber/talc system (♦) original data and (◊) corrected data.

the plastic zone and its length becomes $(a + r_p)$. The elastic stress field ahead of the crack is therefore assumed to be identical to the stress distribution of a real crack length a with the extent of the plastic zone $2r_p$. For $r_p < a$ Equations 3 and 4 are still valid where small increments of r_p values are added to the original crack length a until the data gives minimum deviation from a straight line fit calculated by the least squares method. Fig. 7 shows a typical plot of $U_{\max}$ versus $BD\phi$ where the plasticity effect causes non-linearity in the plot, and also the corrected data of the same where the plastic zone correction factor has been used and the slope of the plot gives the required G_c. Each datum on the plot represents the average of six to eight measurements.

To obtain the fracture toughness K_c, maximum load (P_c) on the load-displacement curve was used to calculate the gross stress at fracture, σ_c, and K_c was calculated from the relationship:

$$K_c = \sigma_c Y a^{1/2} \tag{5}$$

where Y is a geometric finite width correction factor which may be calculated for any shape of specimen [24] and a is the crack length. Fig. 8 shows a plot of σY versus $a^{-1/2}$ where the resulting slope gives the fracture toughness K_c.

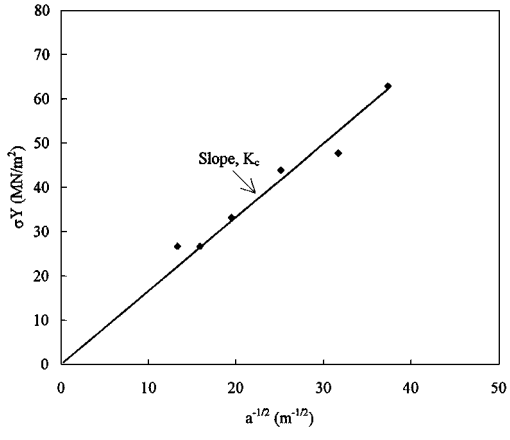

Figure 8 σY versus a$^{-1/2}$ for 2.7% paint (63 μm) in PP/rubber/talc system.

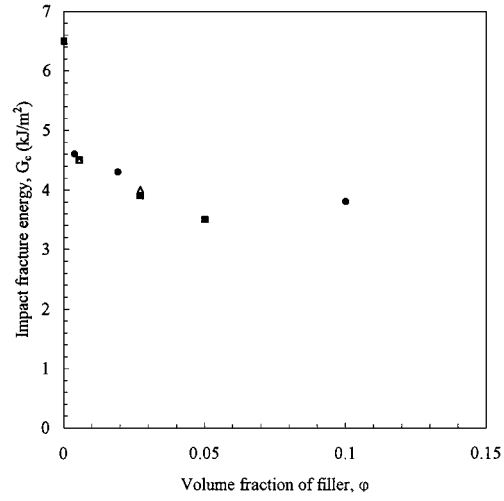

(a)

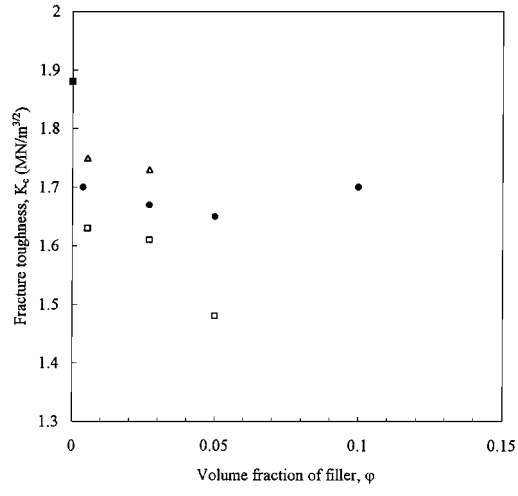

(b)

Figure 9 (a) Impact fracture energy versus volume fraction of (●) glass bead, (□) paint (63 μm) and (Δ) paint (135 μm) filled PP/rubber/talc system. (b) Fracture toughness versus volume fraction of (●) glass bead, (□) paint (63 μm) and (Δ) paint (135 μm) filled PP/rubber/talc system.

It was observed that both G_c and K_c decreased with increasing filler content as shown in Fig. 9. As the adhesion between filler particles and matrix is poor, the fillers become detached from the polymer. Thus the composite fractures as a weak foam, and the fracture energy of the matrix is additionally reduced with increasing filler fraction. The experimental results of Kendall [25] on colloidal silica filled low density polyethylene and poly(methylmethacrylate), of Friedrich and Karsch [26] on silicon dioxide filled polypropylene, of Nabi and Hashemi [27] on glass bead filled acrylonitrile/styrene/acrylate and of Wong and Truss [28] on flyash filled polypropylene were of similar nature and lead to further support of the results. In general the presence of filler could either have a toughening or a weakening effect. On the one hand, fillers tend to increase fracture energy by increasing surface area of fracture due to increase in surface roughness and interaction between the crack front and the dispersed phase for brittle matrix when filler matrix adhesion is poor. On the other hand, they tend to inhibit plastic deformation by constraints or simply by volume replacement, thus reducing the fracture energy. Thus, a

competition exists between these two, and the toughening of the composite depends on which of the two mechanisms predominates. From the results obtained here, it appears that it is the latter mechanism that controls the system. At higher volume fraction of glass beads (10 vol %) there was slight increase in G_c values which might be for localized crack blunting. No such increase was observed for paint particles up to the concentration level examined.

The values of G_c and K_c for the different sized paint particles were little affected at a constant volume fraction of filler with the larger sizes having slightly higher values.

In addition to all the points discussed, the crystalline morphology of the composites may have been influenced by the paint or glass particles which in turn might affect the mechanical properties. This can be revealed by studying the thermal behaviour and using optical microscopy which was beyond the scope of the present investigation.

3.5. Fractography

The fractured specimens were studied to observe the adhesion between filler and matrix. A Hitachi Scanning Electron Microscope, model S520 was used for this purpose. The samples were sputter coated with gold prior to scanning.

Fig. 10 shows the fractured surfaces of (a) paint and (b) glass filled systems. Poor bonding between the glass and the matrix was evident by the smooth appearance of glass surfaces and no matrix adhesion to the surface of the pulled out glass spheres. The irregular paint particles also did not show any bonding with the matrix and created clear voids when being separated from the matrix. These observations support the conclusions drawn in the earlier sections.

Though no effort was made to improve the adhesion between the matrix and the dispersed phase, it was found in the literature that bonding agents do increase the interfacial adhesion between the phases. Young *et al*. [17] studied hybrid composites containing epoxy/rubber/glass (with and without silane coating) systems, and the micrographs of the fractured surfaces showed that the glass particles were more firmly bonded to the matrix with the use of silane bonding agent. They observed that in some instances, a layer of material containing rubber particles was bonded to the glass particles, inhibiting debonding and thus increasing the efficiency of the crack pinning mechanism and the yield stress over the untreated system.

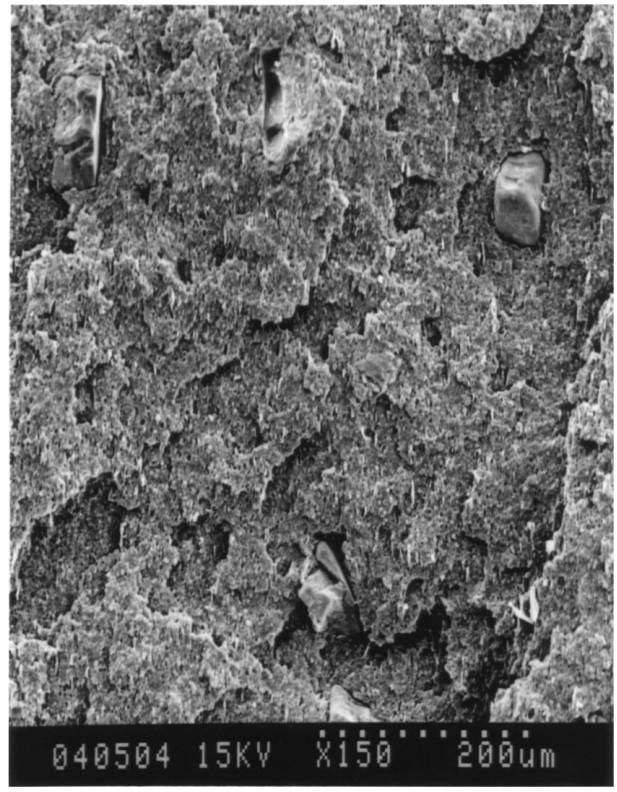

(a)

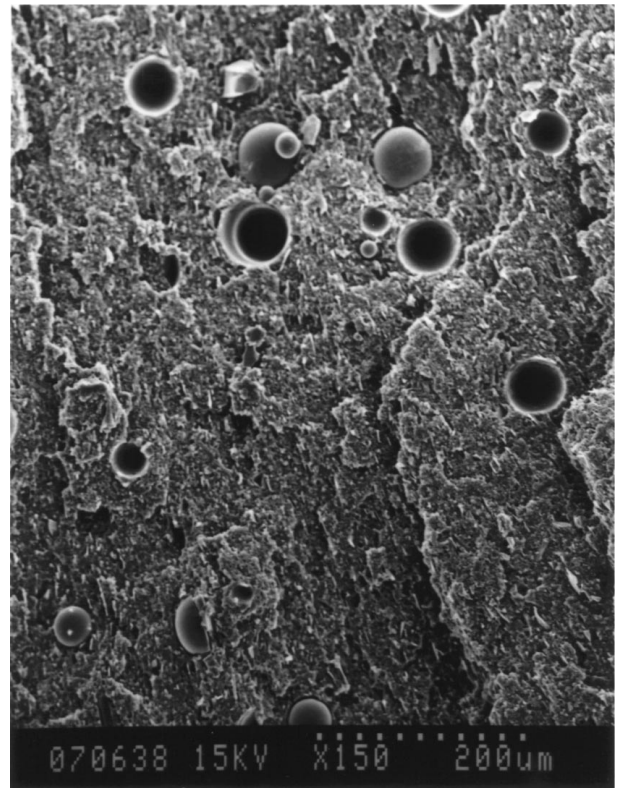

(b)

Figure 10 (a) Scanning electron micrograph of fracture surface of 0.054% paint (135 μm) filled PP/rubber/talc system. (b) Scanning electron micrograph of fracture surface of 1.9% glass filled PP/rubber/talc system.

4. Relationship between mechanical properties and morphology of PP/rubber/filler hybrids

The study of the mechanical properties of the composites are important since it gives an insight into the material characteristics. Mechanical properties of multicomponent systems depend on component properties, their miscibility and processing conditions. For PP/rubber/filler systems, mutual miscibility and adhesion of the components are the crucial factors influencing structure and properties.

In previous works [12–15, 29] three microstructures for three component thermoplastic/elastomer/filler

systems were presented: (a) a separated microstructure where elastomer particles and filler are independently dispersed in polymer matrix (b) a core-shell microstructure where rubber particles with filler core are distributed in matrix and (c) a microstructure of mixed (a) and (b).

The PP/rubber/filler matrices studied in this work had a separated microstructure as shown in Fig. 10 where rubber (tiny dark holes), talc (small white flakes) and glass or paint particles were separated in the polymer matrix, showing poor interfacial adhesion and no affinity to any phases in the composite. This was obtained by extruding all the components together as described in section 2.2. No effort was made to improve the adhesion or miscibility between polymer and filler or polymer and elastomer. Similar observations were cited by Shanks and Long [14] for PP/rubber/talc hybrid where both separated and core-shell microstructure were studied with clear distinction between them.

The experimental results showed that the PP/rubber/talc matrix had a higher modulus than the PP or PP/rubber matrix, as it is well known that modulus is increased by rigid particles and decreased by elastomers. But when glass beads and paint particles were incorporated into the system a decrease in modulus was observed. This was attributed to poor bonding between the matrix and the filler. A decrease in strength and elongation was also observed. Usually, elongation is increased by elastomers and decreased by fillers. In this study, both talc and paint or glass particles restricted the polymer to provide strength between packed particles, and also the particles that do not bond well to the polymer caused cavitation.

The toughening mechanisms activated by rubbery particles and rigid particles are also different. The elastomer particles enhance the extent of shear yielding deformations in the polymer matrix at the crack front due to interaction between the stress field ahead of the crack and the rubbery particles, thus increasing the fracture energy [30–32]. In the case of rigid particles, the toughening mechanism has been mainly ascribed to a crack pinning mechanism, where the particles act as obstacles that pin the crack and cause the crack front to divert between them. Furthermore, increased toughness by rigid inclusions has to meet the conditions of small particle size and that the number is less than the number of particles that can be fully packed into the matrix.

In this study, the PP/rubber/talc matrix had higher fracture energy than the neat PP and the binary PP/rubber system, as both the toughening mechanisms act simultaneously. Martinatti and Ricco [29] investigated the PP/rubber/filler (calcium carbonate and talc) system and observed that in certain ranges of compositions, the inclusions of the secondary phase produces optimization of the impact fracture properties compared to the corresponding binary system. Their results for the ternary system with rubber content of 5% and 16 vol % showed a broad maximum for the total energy required to fracture a specimen and the maximum energy on the load time curve, with about 4 vol % of talc inclusions. Hence, the fracture energy of the ternary blend PP/16 vol % rubber/4 vol % talc was greater than in the corresponding binary systems. No such comment can be made here, as only one combination of PP/rubber/talc was used in this work. But the ternary blend of PP/rubber/talc indeed had a higher fracture energy than the corresponding PP/rubber system. For the composites with inclusions of glass and paint particles, a reduction in fracture energy was observed compared to the base PP/rubber/talc matrix, implying that the toughening mechanism was impaired by the presence of this secondary phase. The inclusions inhibit plastic deformation of the matrix, and because of poor bonding between filler and matrix there is little possibility of stress transfer from polymer to filler, thus giving a weaker structure. The micrographs suggest that the paint and glass particles debond at the matrix inclusion interface. Low adhesion is considered to impair the efficiency of the crack pinning mechanism.

5. Conclusions

The mechanical properties like tensile strength, strain at break, modulus, impact strength, and fracture toughness for the PP/rubber/talc system were all influenced by the addition of fillers such as paint particles and glass beads. Tensile strength decreased linearly according to Piggott and Leinder's equation. Irregular paint particles offered greater stress concentrations, thus reducing strain at break drastically at lower volume fraction, compared to the glass beads where the decrease was gradual. The tensile strength and strain at break was less influenced by the size of paint particles, whereas a slight decrease in the modulus values were observed with decreasing particle size. The impact strength and fracture toughness also decreased with increase in filler concentration. Poor adhesion and absence of stress transfer between matrix and filler are the key factors for these observations. The size of the paint particles had little effect on the impact strength and fracture properties at the filler concentration levels used in this investigation.

References

1. V. MIRANDA, F. S. LAI and R. L. FERDINAND, *Antec* (1994) 2888.
2. YU LONG, B. E. TIGANIS and R. A. SHANKS, *J. App. Polym. Sci.* **58** (1995) 527.
3. J. H. REEVES, *Polymer Age* **6** (1975) 420.
4. M. SUMITA, T. OOKUMA, K. MIYASAKA and K. ISHIKAWA, *J. Mater. Sci.* **17** (1982) 2869.
5. *Idem., Ibid.* **18** (1983) 1758.
6. F. RAMSTEINER and R. THEYSOHN, *Composites* **15** (1984) 121.
7. K. FREIDRICH and U. A. KARSCH, *Fibre Sci. Technol.* **18** (1983) 37.
8. T. J. HUNTLEY and M. W. DARLINGTON, *Polym. Comm.* **25** (1984) 226.
9. S. F. XAVIER, J. M. SCHULTZ and K. FRIEDRICH, *J. Mater. Sci.* **25** (1990) 2411.
10. *Idem., Ibid.* **25** (1990) 2421.
11. *Idem., Ibid.* **25** (1990) 2428.
12. J. JANCAR and A. T. DIBENEDETTO, *J. Mater. Sci.* **30** (1995) 1601.
13. *Idem., Ibid.* **30** (1995) 2438.
14. YU LONG and R. A. SHANKS, *J. App. Polym. Sci.* **62** (1996) 639.

15. *Idem., Ibid.* **30** (1996) 1877.
16. M. R. PIGGOTT and J. LEINDER, *J. App. Polym. Sci.* **18** (1974) 1619.
17. R. J. YOUNG, D. L. MAXWELL and A. J. KINLOCH, *J. Mater. Sci.* **20** (1985) 4169.
18. S. N. MAITI and K. K. SHARMA, *J. Mater. Sci.* **27** (1992) 4605.
19. S. N. MAITI and P. K. MAHAPATRO, *J. App. Polym. Sci.* **42** (1991) 3101.
20. K. GHOSH and S. N. MAITI, *Ibid.* **60** (1996) 323.
21. R. N. TH. VOLENBERG and D. HEIKENS, *J. Mater. Sci.* **25** (1990) 3089.
22. E. PLATI and J. G. WILLIAMS, *Polym. Eng. Sci.* **15** (1975) 471.
23. G. R. IRWIN, *Appl. Mats. Res.* **3** (1964) 65.
24. D. P. ROOKE and D. J. CARTWRIGHT, "Compendium of Stress-Intensity Factors," (HMSO, London, 1976).
25. K. KENDALL, *J. Briti. Polym.* **10** (1978) 35.
26. K. FRIEDRICH and U. A. KARSCH, *J. Mater. Sci.* **16** (1981) 2167.
27. Z. U. NABI and S. HASHEMI, *ibid.* **31** (1996) 5593.
28. K. W. Y. WONG and R. W. TRUSS, *Comp. Sci. Tech.* **52** (1994) 361.
29. F. MARTINATTI and T. RICCO, *ibid.* **29** (1994) 442.
30. A. J. KINLOCH, S. J. SHAW, D. A. TOD and D. L. HUNSTON, *Polymer* **24** (1983) 1341.
31. A. J. KINLOCH, S. J. SHAW and D. L. HUNSTON, *Polymer* **24** (1983) 1355.
32. J. N. SULTAN and F. J. MCGARRY, *Polym. Eng. Sci.* **13** (1973) 29.

Received 24 April
and accepted 28 July 1998